Technical Sciences, 2016, 19(2) 165–187

Quarterly peer-reviewed scientific journal
ISSN 1505-4675
e-ISSN 2083-4527
TECHNICAL SCIENCES
Homepage: www.uwm.edu.pl/techsci/

A NEW APPROACH FOR OBTAINING THE GEOMETRIC PROPERTIES OF A GRANULAR POROUS BED BASED ON DEM SIMULATIONS

Wojciech Sobieski, Waldemar Dudda, Seweryn Lipiński

Department of Mechanics and Basics of Machine Construction
University of Warmia and Mazury in Olsztyn

Received 17 July 2015, accepted 23 February 2016, available online 13 June 2016

K e y w o r d s: granular beds, spatial structure, Discrete Element Method, PathFinder code.

A b s t r a c t

In the article, a new way for obtaining a set of geometrical parameters of granular porous beds is presented, if the data on the locations and sizes of all particles is available. The input data were prepared with the use of Discrete Element Method. The other way for acquiring the input data may be the application of Computed Tomography (CT) and Image Analysis (IA) techniques. All geometrical parameters are calculated with the use of own numerical code called PathFinder (freely available in the Internet together with its source code). In addition to description of the method of calculations, two examples of its use are presented. One simulation was performed in PFC^{3D} code, and the other in YADE software. The aim of the article was to show clearly that a porosity is not sufficient to describe the spatial structure of a porous body. In both presented examples, the porosity value is almost the same, but other parameters, e.g. tortuosity, are different. The motivation to write the PathFinder code were significant problems with obtaining geometrical parameters needed in investigations related to granular porous media. The issues described in the article are a part of an overall research methodology relating to the linking the micro- and macro-scale investigations of granular porous beds. The areas of applications of this methodology are not discussed in the article.

Introduction

In the investigations of fluid flows through porous media, two basic concepts can be distinguished. In the first approach, the porous medium is treated as a matter, which causes flow resistance, and, in a consequence, the

Correspondence: Wojciech Sobieski, Katedra Mechaniki i Podstaw Konstrukcji Maszyn, Uniwersytet Warmińsko-Mazurski, ul. M. Oczapowskiego 11, 10-957 Olsztyn, phone: +48 89 523 32 40, e-mail: wojciech.sobieski@uwm.edu.pl.

pressure drop along the flow direction. In the simplest variant of this approach, it is not important, what is the source of the flow resistance – the global effect is what counts. This is the oldest way for describing or predicting the pressure drop in real flow systems. The Darcy law (DARCY 1856) was the first law in this field and is still one of the most important laws in the porous media research area. In the following years other laws were formulated, like for example the Forchheimer law (1901) (WHITAKER 1996), which expand the range of flows that are possible to be modelled, but the idea was the same all the time. More information about Darcy and Forchheimer laws, as well as the discussion of ranges of their application, can be found for example in the article (SOBIESKI, TRYKOZKO 2011). The main disadvantage of the first approach is the difficulty of connecting the general macro-scale effect (the pressure drop) with the phenomena taking place in the micro-scale (the energy losses due to the friction). Many mathematical models can be found in publications, where such interactions between both scales are sought. The Kozeny-Carman law (KOZENY 1927, CARMAN 1997), Ergun law (ERGUN 1952), Ergun-Wu law (WU et al. 2008), Comiti (COMITI, RENAUD 1989), Barree-Conway law (WU et al. 2011, ZHANG 2013) and other laws can be used as examples. The probability theory and fractal theory are quite popular too. These investigations show the main tendency: from macro-scale to micro-scale.

The second approach is focusing on the physical side of the problem. Here the physical phenomena occurring in the channels inside porous media are most important. The friction (and hence the geometry of these channels) plays the key role in the discussed approach. The importance of this approach increased significantly when the methods of Computational Fluid Dynamic (CFD) became widely available. Thus, the full Navier-Stokes or Reynolds equations may be used for predicting the fluid behaviour in porous zone for many kinds of porous media. Currently, many researchers are trying to understand the processes on micro-scale and their impact on the behaviour in macro-scale. In this approach, the research path leads from micro-scale to macro-scale.

In the current article a new look on the problem in context of granular porous beds (porous media consisting of spherical or quasi-spherical particles) is proposed. In this approach, the research methodology includes three main stages (Fig. 1):

– Acquiring in micro-scale information about the size and location of each particle forming a porous bed.

– Basing on these data, calculating the porosity, tortuosity, specific surface of the porous body and other parameters that can macroscopically characterize the pore space of this type of media.

– Calculating the linear and non-linear terms of macro-scale laws (e.g. Kozeny-Carman law), basing on the structure analyzed at the micro level.

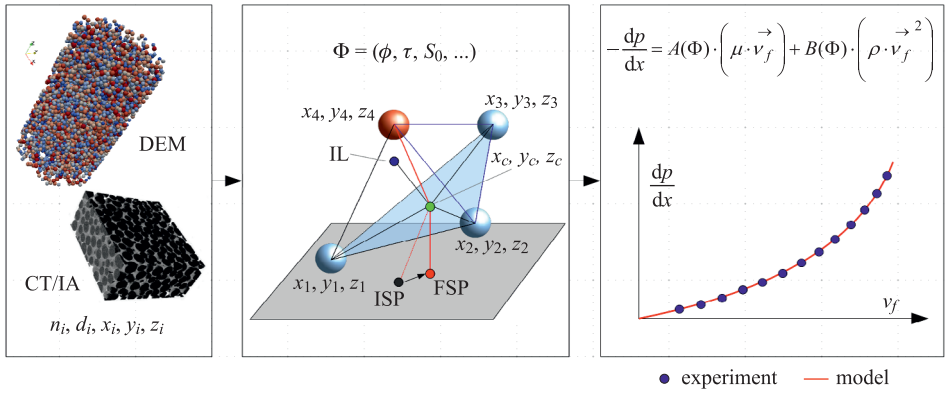

Fig. 1. Schematic representation of the overall research methodology

The realization of the first stage is possible in two ways. The first way is to carry out computer simulations using Discrete Element Method (DEM). In this method all needed data can be obtained directly, through a proper record of the results of the calculations in files. This very method is used in hereby article. The second way is the use of Computed Tomography and the Image Analysis. In this method all needed data can be achieved by appropriate algorithms of image processing which allows to transform a series of CT images into knowledge about the spatial structure of the porous bed.

To calculate a set of geometrical parameters characterizing the spatial structure of porous beds, new algorithms were needed. They were developed first (details in the research report, SOBIESKI 2009a) and then the PathFinder code (*The PathFinder Project*. Online) was written. The current article presents mainly this part of the proposed research methodology.

Having established the information about the spatial structure of the porous bed, the third stage may be started with the creation of a macro-scale model. In the applied methodology the general Forchheimer law is used, but there may be used any different law. This law was implemented to the ANSYS Fluent CFD code by using the so-called Porous Media Model (Fluent Inc.: Fluent 6.3 User's Guide, Chapter 7.19: Porous Media Conditions, September 2006, Fluent Inc.: Fluent 6.3 Tutorial Guide. September 2006, SOBIESKI 2010) and the User Defined Functions (UDF). In this way a full control of the model is provided and all spatial parameters may be introduced as constant values or functions dependent on the location or time.

The general set of input data for macro-scale laws

Many laws for calculating the pressure drop in fluid flow systems with porous media can be shown in a unified form (SOBIESKI, TRYKOZKO 2011, 2014a, b):

$$\frac{\mathrm{d}p}{\mathrm{d}x} = A(\Phi) \cdot (\mu \cdot \vec{v}_f) + B(\Phi) \cdot (\rho \cdot \vec{v}_f) \tag{1}$$

where:
p – pressure [Pa],
x – a coordinate along which the pressure drop occurs [m],
$A(\Phi)$ and $B(\Phi)$ – two generalized parameters, dependent on the set Φ characterizing the spatial structure of the porous medium,
μ – dynamic viscosity of the fluid [kg/m · s)],
ρ – density of the fluid [kg/m^3)],
$\vec{v}_f$ – filtration velocity [m/s].

The commonly used Kozeny-Carman equation may serve as an example of a law with the structure like the one in formula (1). This equation is derived for calculating the permeability of well-sorted sand (NEETHIRAJAN et al. 2006, FOURIE et al. 2007), in which coefficients $A(\Phi)$ and $B(\Phi)$ have the following forms:

$$\begin{cases} A(\Phi) = \dfrac{1}{\kappa} = C_{\mathrm{KC}} \cdot \tau_f \cdot S_0 \cdot \dfrac{(1-\phi)^2}{\phi^3} \\ B(\Phi) = 0 \end{cases} \tag{2}$$

where:
κ – permeability [m^2],
C_{KC} – Kozeny-Carman pore shape factor (a model constant), which should be equal to 5.0 (CARMAN 1997) [–],
τ_f – the tortuosity factor [m^2/m^2] defined as the square of the tortuosity τ [m/m],
S_0 – specific surface of the porous body [1/m],
ϕ – porosity [m^3/m^3].

It should be noted that researchers have also used other forms of Kozeny-Carman equation (DUNN 1999, RAINEY et al. 2008, RESCH 2008, ROSSEL 2004). A larger discussion on this topic was presented in the work (SOBIESKI 2014).

Another known law, matching formula (1), is the Ergun equation (ERGUN 1952, NIVEN 2002, HERNÁNDEZ 2005, DUNN 1999), in which:

$$\begin{cases} A(\Phi) = 150 \cdot \dfrac{(1-\phi)^2}{\phi^3 \cdot (\psi \cdot d)^2} \\ B(\Phi) = 1.75 \cdot \dfrac{(1-\phi)}{\phi^3 \cdot (\psi \cdot d)} \end{cases} \tag{3}$$

where:

d – the representative (e.g. average) diameter of particles forming a porous bed [m],

ψ – sphericity coefficient [–] (less than 1 in general and equal to 1 when the particles are spherical in shape, SOBIESKI 2009b).

In the literature one can find many other formulas for $A(\Phi)$ and $B(\Phi)$ coefficients (e.g., MIAN (1992), SKJENTE et al. (1999), SAMSURI et al. (2000), BELYADI A (2006), BELYADI (2006), LORD et al. (2006), AMAO (2007), Wu and Yu (WU et al. 2007), but almost all of them are related to the geometrical structure of the porous media.

The mathematical forms of physical laws cited here are not very important in this article and they serve only as examples. The most important is the fact, that usually only a few basic geometrical parameters are needed for modelling the fluid flows through porous beds. Such set may be also defined as follows:

$$\Phi = \{d, \phi(V_p,V),\ \varepsilon(V_s,V),\ \tau(L_p,L_0),\ S_0(S_s,V_s,V),\ \psi(l_x,l_y,l_z)...\} \tag{4}$$

where:

V_p – the total volume of the pore part of a porous medium (filled by a fluid) [m^3],

V_s – the total volume of all particles in the bed [m^3],

V – the total volume of a porous medium [m^3],

L_p – the length of a flow path [m],

L_0 – the depth of the porous medium in the main flow direction [m],

S_s – the total inner surface of a solid body [m^2],

l_x,l_y,l_z – the particle size in three directions of the space [m].

Having established the parameters of set Φ, both $A(\Phi)$ and $B(\Phi)$ terms may be calculated, according to the formulas (2), (3) or others. Of course, the parameters set can be used for other purposes.

It is worth noting, that some parameters of the Φ set can be obtained very easily (assuming that the data with locations and sizes of all particles is available). Others, in turn, are very difficult to determine. It would be advantageous to have a convenient tool that allows obtaining all the information. The PathFinder numerical code is created to be such a tool. In the work (SOBIESKI et al. 2012) the method of tortuosity calculation was shown. In the current article, a newly developed version of this algorithm is described as well as other parts of the whole calculation algorithm implemented into the PathFinder code. In authors' opinion, this new numerical code may be very useful for the researchers dealing with granular porous media – especially, that the PathFinder software is freely available in the Internet together with the source code (*The PathFinger Project*. Online).

The calculation methods

The PathFinder code

The PathFinder software is intended for calculating a set of geometrical parameters of a porous bed, when the data with locations and sizes of all particles is available. PathFinder in fact is only a solver and the visualization should be made in Gnuplot environment (Gnuplot Home Page. Online) (during calculations) or in ParaView software (ParaView Home Page. Online) (after calculations). PathFinder automatically generates suitable output files for that purpose, in a form of a simple text, in VTK or CSV formats, as well as shell scripts for an operating system. Using other, additional applications for the results visualization is possible, too (e.g. The MayaVi Data Visualizer. Online).

The PathFinder software works with a text file with five columns which contain information in the following order: consecutive numbers of each sphere, X, Y and Z-coordinates of centres of spheres and diameters of spheres. The X and Y columns may be swapped, but the Z column must be always the fourth. This is important because it is assumed that this is the main flow direction. In data reading process, every line is considered as a new particle, so the number of lines gives information about the bed size.

For PathFinder it is not relevant in which way the input file was generated: using either results of the Discrete Element Method (DEM) simulation or the results of Computed Tomography and the 3D Image Analysis. In the present article two examples from the first variant are used (Fig. 2). The left figure presents a cylindrical domain with 18188 particles (DEM simulation was made in PFC^{3D} code, ITASCATM Home Page. Online) and the right a cuboid domain

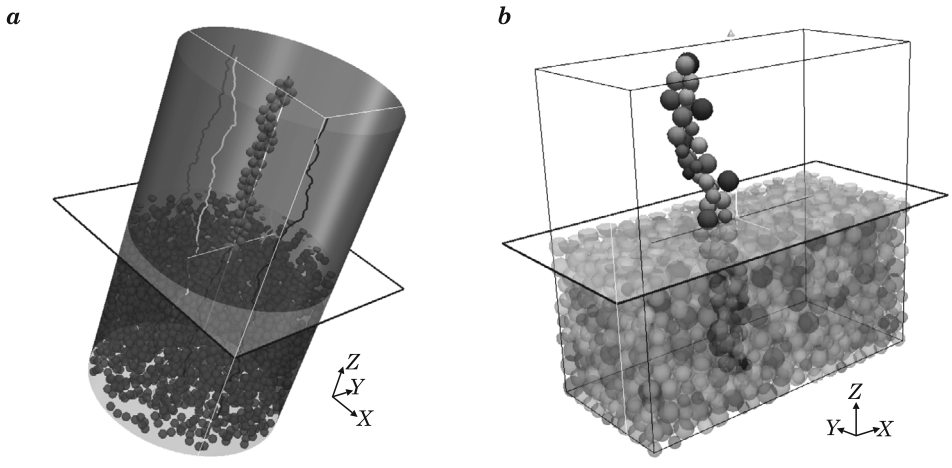

Fig. 2. Examples of visualisation the results obtained in the FathFinder code

with 4000 particles (DEM simulation was made in YADE code, YADE Home Page. Online). In both examples, a central path with surrounding particles is shown.

Calculating the domain range

Under the expression „calculation domain", a virtual space is meant here, where all calculations take place. Usually the domain volume is the same as the bed volume.

All spheres in the bed are described by 5 variables: n_i – number of the i-th sphere; x_i – X coordinate of the i-th sphere centre; y_i – Y coordinate of the i-th sphere centre; z_i – Z coordinate of the i-th sphere centre; d_i – diameter of the i-th sphere. The total number of spheres in the bed is denoted by n_s.

In the first step, all spheres are sorted by the Z coordinate. In this way, the sphere lying lowest in the bed has the index $i = 1$ and the highest sphere index is $i = n_s$. In determination of the Z-axis range, the particle diameters are taken into account (Fig. 3):

$$z_{\min} = \min\left(z_i - \frac{1}{2} \cdot d_i\right),\ z_{\max} = \max\left(z_i + \frac{1}{2} \cdot d_i\right) \tag{5}$$

Note, that if the bottom surface of the bed is horizontal and flat, many particles have the lowest surface point in the same XY plane. In the same way the ranges of X and Y axis are calculated.

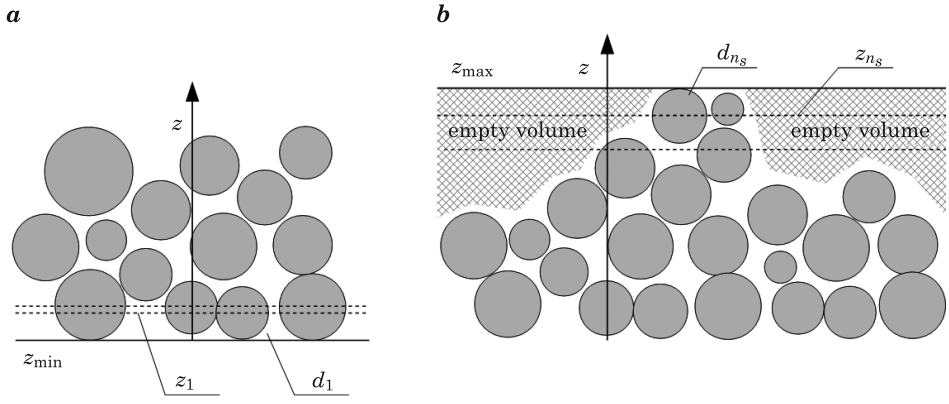

Fig. 3. Calculating the location of the bottom and top surface of the bed

In real beds, the bottom and the lateral surfaces usually limit the locations of particles. However, the top surface can be uneven and some particles may protrude from the bed. In this case, „empty volume" in the bed exists, what may give inaccuracies in calculations. To avoid this, all protruding particles should be rejected from the calculations (Fig. 4). As a result, the volume of the calculation domain is a little less than the real bed volume. The number of rejected particles is described by variable n_{s_rej}. Also, notice the small particle right to the particle determining the height of the bed (before discarding protruding particles). Despite the fact that it has the highest value of Z coordinate, it is not recognized by the algorithm as the highest sphere in the bed due to its small diameter.

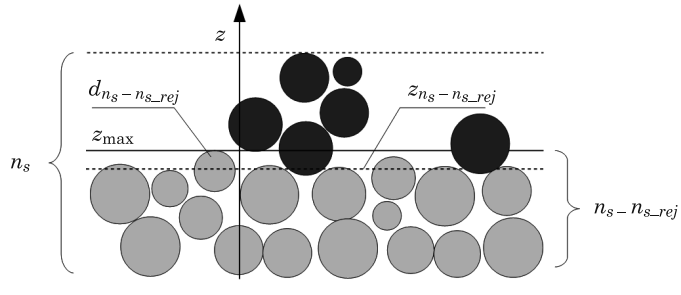

Fig. 4. Visualization of the idea of rejecting protrudes particles: the empty volume is not taken into account

Calculating the default Initial Starting Point

The default Initial Starting Point (ISP), from which the algorithm starts, is calculated as

$$x_0 = x_{\min} + \frac{x_{\max} - x_{\min}}{2},\ y_0 = y_{\min} + \frac{y_{\max} - y_{\min}}{2},\ z_0 = z_{\min} \tag{6}$$

where index 0 denotes the ISP. In the PathFinder source code, the same variables are then used for the Final Starting Point (FSP).

Calculating the domain height

The domain height is calculated as

$$L_0 = z_{n_s - n_{s\_rej}} + 0.5 \cdot d_{n_s - n_{s\_rej}} - z_{\min} \tag{7}$$

where:
L_0 – the height of the calculation domain [m],
$z_{n_s - n_{s\_rej}}$ – the Z coordinate of the highest used in calculations sphere in the bed [m],
$0.5 \cdot d_{n_s - n_{s\_rej}}$ – the radius of the highest used in calculations sphere in the bed [m].

Calculating the domain volume

In the PathFinder code, calculations can be performed in porous beds (domains) in cuboid and cylindrical shapes. In the cases when the source geometry is complex (in DEM models or when the objects are scanned with the use of the CT technique), a representative part of the porous bed with an appropriate shape must be exported for the PathFinder needs.

In the case of a cuboid shape the volume of the domain is calculated from the following formula:

$$V = (x_{\max} - x_{\min}) \cdot (y_{\max} - y_{\min}) \cdot L_0 \tag{8}$$

When the porous bed has a cylindrical shape, the domain volume is calculated as follows:

$$V = \frac{\pi \cdot d_{cyl}^2}{4} \cdot L_0 \tag{9}$$

where:
d_{cyl} is the diameter of the cylinder [m],

calculated as the average range of X and Y axis:

$$d_{cyl} = \frac{1}{2}\left[(x_{\max} - x_{\min}) \cdot (y_{\max} - y_{\min})\right] \tag{10}$$

Calculating the tortuosity

Tortuosity is the ratio of the actual length of flow path to the physical depth of a porous bed:

$$\tau = \frac{L_p}{L_0} \tag{11}$$

where:
τ – the tortuosity [m/m],
L_p – the length of a flow path [m].

Note, that the tortuosity may be interpreted as a geometrical parameter: the length of a typical pore channel (which is independent of the filtration velocity) or as a flow parameter: the length of a typical fluid stream (which is dependent on the filtration velocity). In the PathFinder code only the geometrical tortuosity may be directly calculated.

The algorithm (so-called Path Tracking Method) for calculating length L_p in PathFinder was described in details in the papers SOBIESKI (2009a), SOBIESKI et al. (2012) and DUDDA, SOBIESKI (2014). Here is the summarized procedure (Fig. 5; particles are not in a scale):

– Arbitrarily choose an Initial Starting Point (ISP) at the bottom of the porous bed (*a*);

– Find three nearest particles to the ISP that form a triangle in the space (*b*);

– Calculate the coordinates of the centre of gravity of the surface (in the triangle plane) through which flows the fluid (this part was changed since the work SOBIESKI et al. 2012 was published) (*c*);

– Move the ISP to the Final Starting Point (FSP) – in this way the first path section is perpendicular to the bottom surface of the bed (*d*);

– Calculate the normal to the triangle, in the direction of Z axis;

– Estimate coordinates of the so-called Ideal Location (IL), in which the next sphere surrounding the path should be located (*e*);

– Move the IL closer to the triangle centre (*f*);

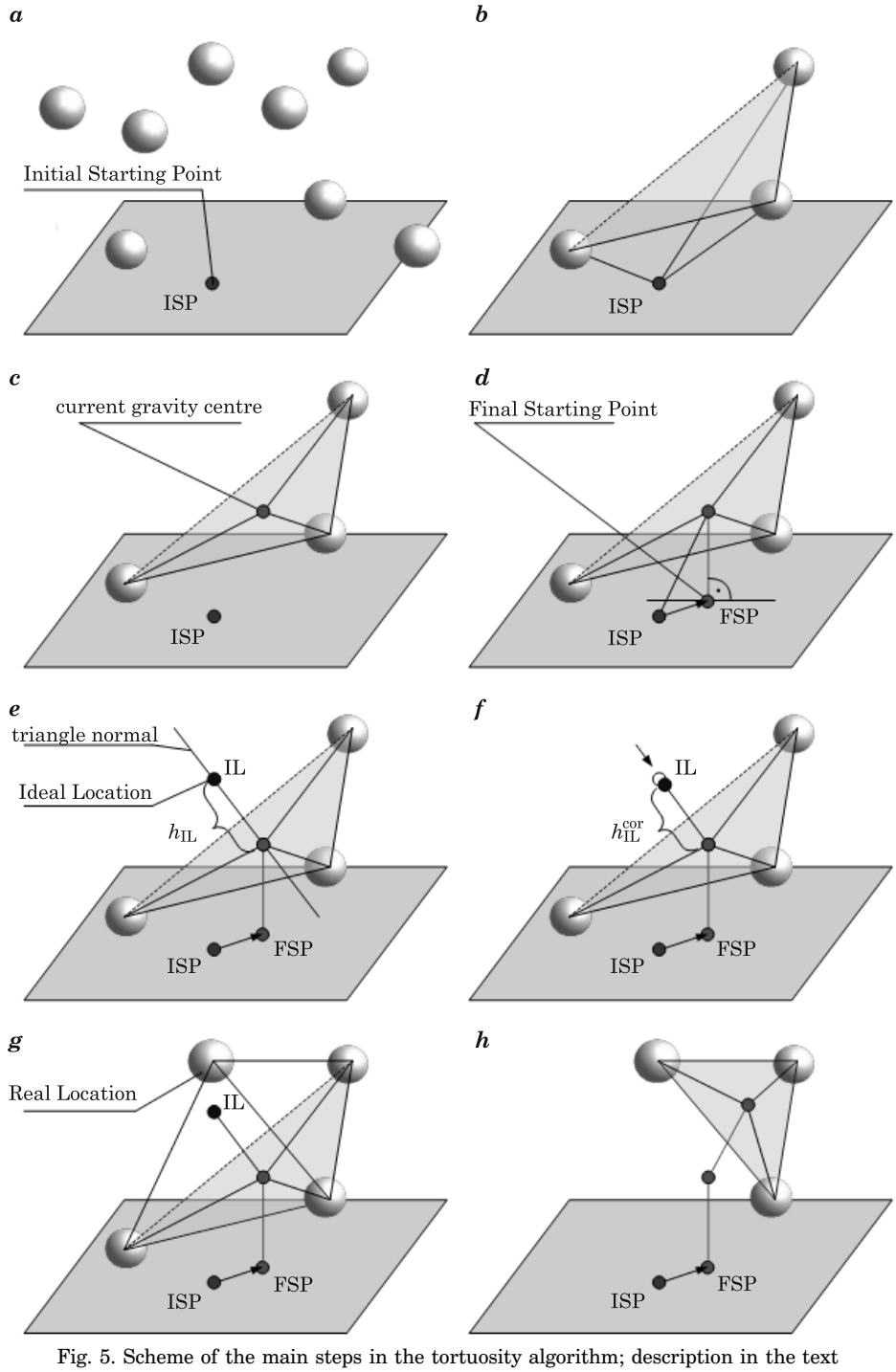

Fig. 5. Scheme of the main steps in the tortuosity algorithm; description in the text

– Find the nearest particle to the IL – this is the Real Location (RL) of the 4-th particle forming tetrahedron in the space (g);

– Remove the lowest sphere from tetrahedron 1-2-3-4 to obtain the base triangle for the next tetrahedron (h);

– Continue the calculations from the third point until reaching the top surface of the bed;

– Calculate the length of the path inside the tetrahedron (a flow path is a line connecting the centroid of the base triangle with the centroid of one of the three side triangles).

The algorithm finishes when the distance between current IL and the nearest particle centre is bigger than the distance between the top surface of the bed and the Z coordinate of the IL. The last section is perpendicular to the top surface of the bed.

The number of path points is higher by two in relation to the number of tetrahedrons used for searching the path sections.

In the PathFinder code an additional algorithm allows to smooth the path exists. Due to this, the path length is a little shorter. The use of the smoothed value is currently not recommended.

Calculation of the triangle centre of gravity

The algorithm for calculating the centre of gravity of the shape, through which the fluid flows, is described in details in the work DUDDA and SOBIESKI (2014). This algorithm consists of two stages. First, the coordinates of all basic figures are calculated (one triangle and three circle segments) and next, the summation method is used to calculate coordinates of the resultant centre of gravity of the set of basic shapes (Fig. 6)

$$x_{gc} = \frac{A_t \cdot x_{tc} - A_1 \cdot x_{s1} - A_2 \cdot x_{s2} - A_3 \cdot x_{s3}}{A_t - A_1 - A_2 - A_3}$$

$$y_{gc} = \frac{A_t \cdot y_{tc} - A_1 \cdot y_{s1} - A_2 \cdot y_{s2} - A_3 \cdot x_{s3}}{A_t - A_1 - A_2 - A_3} \tag{12}$$

$$z_{gc} = \frac{A_t \cdot z_{tc} - A_1 \cdot z_{s1} - A_2 \cdot z_{s2} - A_3 \cdot z_{s3}}{A_t - A_1 - A_2 - A_3}$$

where:

x_{gc}, y_{gc}, z_{gc} – coordinates of the obtained centre of gravity [m],

A_t – the area of the current triangle [m^2],

x_{tc}, y_{tc}, z_{tc} – coordinates of the current triangle centre [m],
$A_{1,2,3}$ – areas of circle segments [m2],
x_s, y_s, z_s – coordinates of gravity centres (denoted by the sign) of circle segments [m].

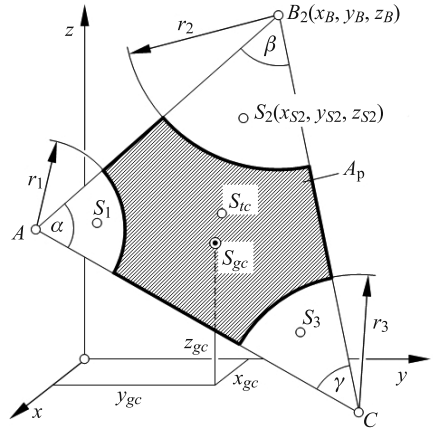

Fig. 6. The shape, through which the fluid flows and its gravity centre

The Ideal Location and its correction

For calculating the Ideal Location, a characteristic dimension is used. It can be the average length of the current triangle sides l_{ave} (recommended) or the average diameter of spheres d_{ave} forming the current triangle. In consecutive calculations it was assumed, that the tetrahedron is regular and all sides have lengths equal to the characteristic dimension. In that case, the height of such tetrahedron may be calculated from the simple formula:

$$h_{\text{IL}} = c_{\text{dim}} \cdot \sqrt{\frac{2}{3}} \tag{13}$$

where:
h_{IL} – the predicted distance between the IL and the triangle plane [m],
c_{dim} – the characteristic dimension [m].

Height h_{IL} is measured on the triangle normal in the direction of increasing values of the Z coordinate.

In real systems, particles forming a triangle may not touch one another, which results is that the fourth particle falling partly between them. In

extreme cases, the fourth particle can slide completely between particles that form the triangle. That can happen when the actual triangle area is three times larger than the area of a triangle with one side equal to the average diameter of the spheres forming the current triangle (derived in SOBIESKI 2009a). If this ratio is higher than 3, a correction algorithm is used (it may be turned off using the settings file) and new three particles close to the current triangle centre are then searched. The number of such corrected triangles is shown in the final report. This normalized critical area of the triangle is also included in the settings file, but impossible to omit entirely.

Usually the area of the real triangle is far from the critical area and the „sinking" effect is small, but not to omit. Therefore, the formula (13) should rather be defined as follows:

$$h_{\mathrm{IL}} = c_{\mathrm{dim}} \cdot h_{\mathrm{cor}} \sqrt{\frac{2}{3}} \tag{14}$$

where:
h_{cor} is a correction coefficient for the Ideal Location [–].

This coefficient may be defined (in the settings file) as a constant value:

$$h_{\mathrm{cor}} = 0.5 \tag{15}$$

or a function:

$$h_{\mathrm{cor}} = f(\mathrm{I_A}) = 1 - \frac{\exp(a \cdot (I_A - b))}{1 + \exp(a \cdot (I_A - b))} \tag{16}$$

where:
I_A – the area indicator [–],
a – a coefficient (obtained in earlier numerical investigations SOBIESKI 2009a) responsible for the function gradient and equal to 8.0 [–],
b – a coefficient (obtained in earlier numerical investigations SOBIESKI 2009a) equal to average value of normalized triangle area for the whole porous bed, with value equal to 0.5 [–].

The area indicator is defied as

$$I_A = \frac{A_i}{A_0} \tag{17}$$

where the current triangle area is calculated from the Heron formula

$$A_i = \sqrt{\frac{L}{2} \cdot \left(\frac{L}{2} - a\right) \cdot \left(\frac{L}{2} - b\right) \left(\frac{L}{2} - c\right)} \tag{18}$$

and the area of the reference triangle A_0 (triangle with all sides equal to the characteristic dimension) as

$$A_0 = \frac{c_{\text{dim}} \cdot \sqrt{3}}{4} \tag{19}$$

Symbols a, b and c in formula (18) denotes lengths of current triangle sides [m].

The details about this issue as well as the way of obtaining all constants are described in a research report (SOBIESKI 2009a), which was written parallel to performing implementation actions. This report contains descriptions of many issues not mentioned in the hereby article and shows the process of creation the final version of the Path Tracking Method.

Calculating the porosity

Having obtained the information about diameters of all particles in the bed, the total volume of all particles in the porous bed can be calculated. This can be done as follows:

$$V_s = \sum_{i=1}^{n_s - n_{s\_rej}} \frac{\pi \cdot d_i^3}{6} \tag{20}$$

where:
V_s – the total volume of all particles in the bed [m^3],
d_i – the diameter of the i-th particle in the bed [m].

Using the formula (8) or (9) and the equation (20), the porosity of the granular bed may be consequently calculated as:

$$\phi = \frac{V_p}{V} = \frac{V - V_s}{V} = 1 - \frac{V_s}{V} \tag{21}$$

Calculating the inner and the specific surface of the solid body

The inner surface of the solid body may be obtained from the following formula (assuming point contacts between particles)

$$S_p = S_s = \sum_{i=1}^{n_s - n_{s\_rej}} \pi \cdot d_i^2 \tag{22}$$

where:
S_p – the total surface of the pore space in the bed [m^2],
S_s – the total surface of all particles in the bed [m^2].

The specific surface of the porous body is calculated in two ways, i.e. according to the Kozeny theory (KOZENY 1927):

$$S_{0,\text{Kozeny}} = \frac{S_p}{V} \tag{23}$$

and to the Carman theory (CARMAN 1997):

$$S_{0,\text{Carman}} = \frac{S_p}{V_s} \tag{24}$$

The relationship between both definitions is as follows:

$$\frac{S_{0,\text{Kozeny}}}{S_{0,\text{Carman}}} = 1 - \phi \tag{25}$$

The approach to the definition of the specific surface of the porous body is one of the differences between the Kozeny equation and the Carman formula.

Calculation examples

In Table 1 there are settings of PathFinder calculations for the two examples previously described. All calculations were made with use of version IV.1 of the PathFinder code.

Table 1

Settings for the calculations in the PathFinder code

Settings	Units	YADE	PFC^{3D}
Number of particles	[–]	4000	18188
Particle diameter	[mm]	31.1 – 57.7	5.5 – 7.5
Domain geometry	[–]	cuboids	cylinder
ISP location	[–]	00	00
ISP x shift	[–]	0.5	0.5
ISP y shift	[–]	0.5	–
Number of rejected particles	[–]	0	19
Triangle center calculating method	[–]	gravity centre	gravity centre
Characteristic dimension	[–]	l_{ave}	l_{ave}
Correction method for the IL	[–]	function	function
Correction coef. for constant method	[–]	0.5	0.5
a parameter for function method	[–]	0.8	0.8
b parameter for function method	[–]	1.3	1.3
Critical area triangle correction	[–]	Yes	Yes
Critical area of the triangle	[–]	3.0	3.0
Smooth the path	[–]	No	No

The number of rejected particles n_{s_rej} for performing coarse calculations should be set to zero. If there is a suspicion of a free space existence (like in the case shown in Fig. 3), this value should be increased. The best way to obtain this parameter is to perform a set of calculations with different n_{s_rej} values and to observe results, particularly the porosity value. A relationship between the number of rejected particles and the porosity value may be prepared here (e.g. in a graphical form). On this basis, the best value of this parameter can be chosen. This method was used for obtaining this parameter for the PFC^{3D} example (SOBIESKI 2009a), in which a free surface of the porous bed exists. In the example from YADE, the number of rejected particles equal zero, due to the way of DEM modelling. All walls were set as flat surfaces, moving closer to each other during calculations. In such a case, no empty area exists in the modelled system. In the PathFinder software, the ISP must be chosen for performing the calculations. The simplest way is to choose ISP directly in the settings file as one from 9 default locations (SOBIESKI 2009a, SOBIESKI et al. 2012, SOBIESKI, LIPIŃSKI online). The description of point location contains two signs (Fig. 7): the first concerns the X axis, the second the Y axis. Both signs may have values: „–" (the negative part of the axis), „0" (zero point of the axis) and „+" (the positive part of the axis). The combination of signs is as follows: +0, + –, 0 –, – –, –0, – +, 0+, ++, 00.

By default, all points surrounding the zero point of X and Y axis are located in the middle of the section connecting the zero point and the domain wall. The distance may be changed by using options x-shift and y-shift available in the settings file. These coefficients may be set between 0 (the ISP is in the zero

point – the middle of the bottom domain wall) and 1 (the ISP is on the wall). The default values for both coefficients are 0.5. This value is not important in the current point, because only one path, from the central point, is calculated.

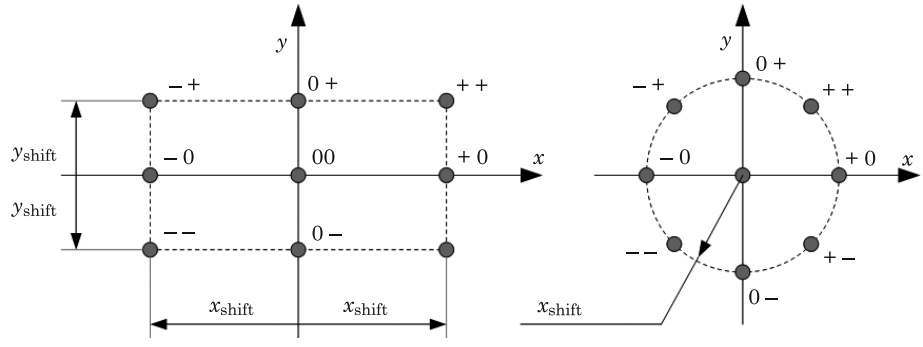

Fig. 7. Default locations of the Initial Starting Point for both possible types of domain

In both examples the recommended values for the characteristic dimension (l_{ave}), the correction method (function) and its coefficients (a and b), the critical area of the triangle, and the method for calculating the triangle centre (gravity centre) were used.

Table 2 contains the calculation results for both test examples. The numbers of path points inform how many of tetrahedral structures were found in the iteration process. In every structure of this kind, one section of the path is located. The number of tetrahedral structures is always lowered by 2. Thus

Table 2

Results of calculations

Settings	Units	YADE	PFC^{3D}
Number of path points	[–]	59	130
Number of path rejected points	[–]	0	0
Number of corrected triangles	[–]	0	0
Bed (domain) height	[m]	0.883302	0.254938
Length of the path	[m]	1.053803	0.317288
Average angle between path sections	[°]	141.557825	139.109342
Tortuosity	[m/m]	1.193026	1.244571
Volume of the bed (domain)	[m^3]	0.345158	0.004505
Inner surface of the solid body	[m^2]	25.534886	2.393343
Specific surface (Kozeny def.)	[1/m]	73.980321	531.227627
Specific surface (Carman def.)	[1/m]	127.652558	915.918417
Volume of the porous body	[m^3]	0.200034	0.002613
Porosity	[m^3/m^3]	0.420456	0.420006
Ergun A	[1/m^2]	343565.12	16372081.72
Ergun 2*B	[1/m]	614.39	4248.07
Kozeny-Carman term	[1/m^2]	524013.00	29498873.86

is due to the fact that the first (FSP) and the last path point are calculated in different way.

During the calculations, it is checked whether there are duplicate points. If yes, one of them is removed from the path and the appropriate information is shown in the final report.

The number of corrected triangles gives information of how many times the corrections based on critical area of the triangle were made (duplicate points may be created in such case). This value should be zero – other values mean that in the bed probably a structural non-continuity exists locally. Sometimes such a case does occur. The importance of other values contained in Table 2 has been already explained.

It should be added here, that the B term in the Ergun law is doubled in the final report. This is because this term must be introduced in this way in the ANSYS Fluent software (Fluent Inc.: Fluent 6.3 User's Guide, Chapter 7.19: Porous Media Conditions, September 2006, Fluent Inc.: Fluent 6.3 Tutorial Guide. September 2006) (but only if the interface is used, not the UDF technique).

PathFinder gives possibility to present results of calculation in a graphical form. The most important visualization may be performed using the ParaView or MayaVi software. Details about the visualisation processes are described in the PathFinder User's Guide (SOBIESKI et al. 2012). In Figure 8 there is the original porous bed created in the PFC^{3D} code (LIU et al. 2008a, b). Additionally the calculation results of the PathFinder code are visible there and these are: five paths, the spheres surrounding the paths, as well as the tetrahedral structures used to obtaining the path sections. The tetrahedron structures may be additionally coloured according to few scalars: values of triangle areas, values of flow areas, values of perimeters (of the triangle, of the flow shape, and of the friction), values of the quality indicators, values of angles between triangle normal and the Z-axis and others. The central path with surrounding spheres and a part of the bed for the YADE example, was shown earlier in Figure 2 (right).

The other way of visualization calculation results is using scripts of the Gnuplot graphical environment. Thanks to them, one can follow the process of calculation. If appropriate option is set in the settings file, the current results may be shown in every iteration (Fig. 9): the Initial Starting Point, the Final Starting Point, the current tetrahedron, the current Ideal Location, the current Real Location, the current triangle and the next triangle. At the end, the current path may be shown. When using the Gnuplot scripts, values of all important variables may be seen, i.e. those being calculated for every tetrahedral structure. Many other Gnuplot scripts are created during such a calculation; most of them are not described here.

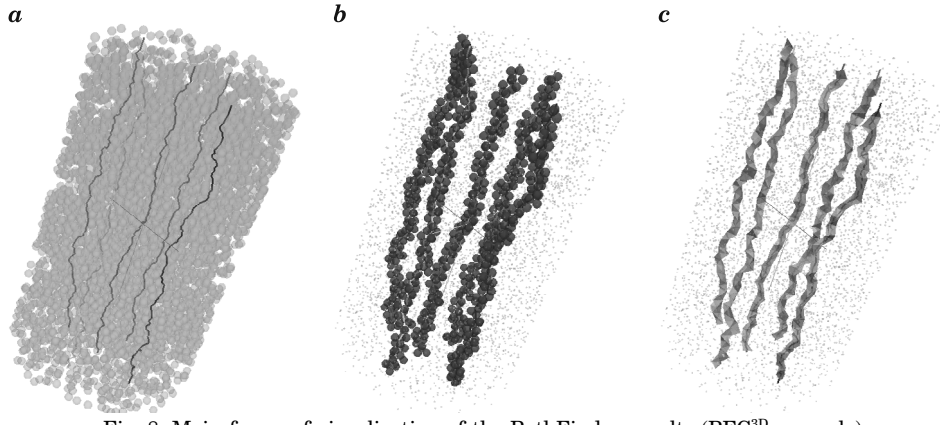

Fig. 8. Main forms of visualization of the PathFinder results (PFC^{3D} example)

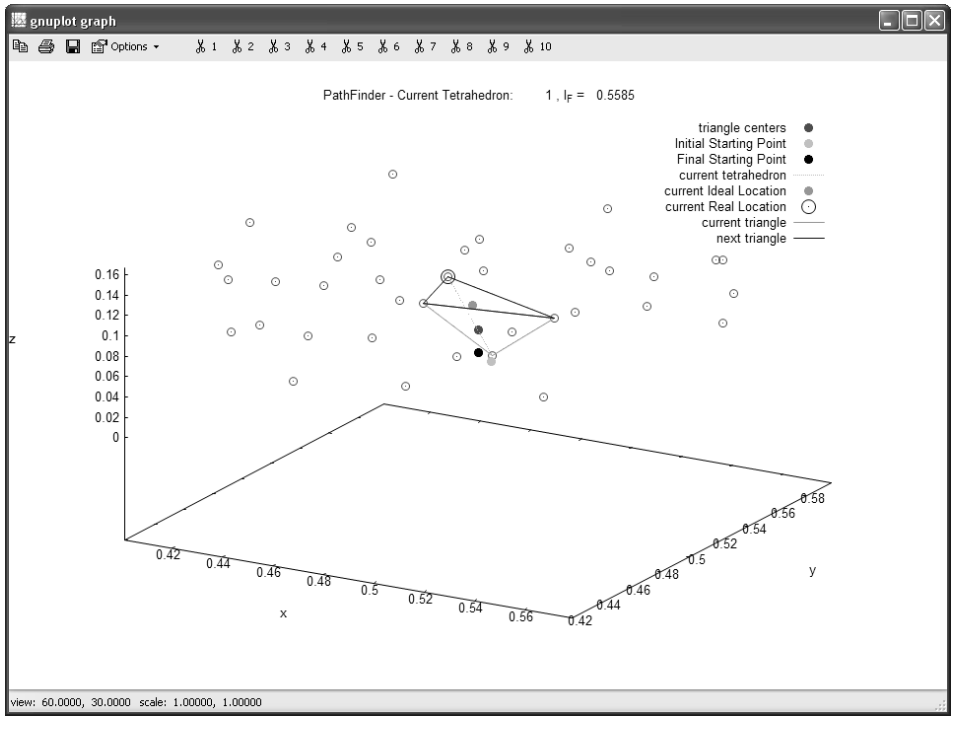

Fig. 9. Visualization of the first tetrahedron in the path (YADE example)

In the current example, only one path for every case is presented (from ISP = 00) due to the desire to show details of a calculation – some results, like the number of path rejected points (duplicates) or the number of corrected triangles must not be averaged. Nevertheless, in general the PathFinder has

appropriate algorithms for automatic calculation of many paths and for comparing or averaging data. For comparison, the average tortuosity calculated for 25 paths (with x-shift and y-shift equal to 0.25, 0.5 and 0.75) is equal to 1.24 for the PFC^{3D} example, and 1.23 for the YADE example. In general it is recommended to calculate more than one path (minimum 5, SOBIESKI 2009a) and use the average value for further calculations.

Summary

The performed works can be summarized as follows:

– The porosity is not a sufficient parameter for describing the spatial structure of a porous bed. In both examples the porosity values were almost the same while other properties were different (e.g. the tortuosity).

– A relationship between tortuosity value and the average angle between path sections can be seen. When this angle is smaller, the tortuosity is higher.

– The tortuosity in the PFC^{3D} example is higher than in the second case, which is caused by the differences in the particle sizes and the diameter distribution. In consequence, the shapes of channels must be more complicated. It can be concluded that the tortuosity value depends on the diameters distribution in the bed.

– The A and B terms are different in both cases. It may stem from the fact that smaller diameters results in turn thinner pore channels. If the pore channel is thinner, the greater is the flow resistance (due to the viscosity).

– The results of calculations described in the article should be compared with other methods: analytical (e.g. porosity-tortuosity correlations available in the literature), numerical (e.g. by the use of the Lattice Boltzmann Methods or the Immersed Boundary Method) and of course experimental. Such investigations are in progress and we will publish their results in the near future.

References

AMAO A.M. 2007. *Mathematical Model For Darcy Forchheimer Flow With Applications To Well Performance Analysis*. MSc Thesis. Department of Petroleum Engineering, Texas Tech University, Lubbock, Texas.

BELYADI A. 2006. *Analysis of Single-Point Test To Determine Skin Factor*. PhD Thesis. Department of Petroleum and Natural Gas Engineering, West Virginia University, Morgantown, West Virginia.

BELYADI F. 2006. *Determining Low Permeability Formation Properties from Absolute Open Flow Potential*. PhD Thesis. Department of Petroleum and Natural Gas Engineering, West Virginia University, Morgantown, West Virginia.

CARMAN P.C. 1997. *Fluid Flow through a Granular Bed*. Transactions of the Institute of Chemical Engineers, Jubilee Supplement, 75: 32–48.

Comiti J., Renaud M.A. 1989. *New model for determining mean structure parameters of fixed beds from pressure drop measurements: application to beds packed with parallelepipedal particles*. Chemical Engineering Science, 44(7): 1539–1545.

Darcy H. 1856. Les *Fontaines Publiques De La Ville De Dijon*. Victor Dalmont, Paris.

Dudda W., Sobieski W. 2014. *Modification of the PathFinder algorithm for calculating granular beds with various particle size distributions*. Technical Sciences, 17(2): 135–148.

Dunn M.D. 1999. *Non-Newtonian Fluid Flow through Fabrics*. National Textile Center Annual Report: C98-P1, Philadelphia University, November.

Ergun S. 1952. *Fluid flow through packed columns*. Chemical Engineering Progress, 48(2): 89–94.

Fluent Inc.: Fluent 6.3 Tutorial Guide. September 2006.

Fluent Inc.: Fluent 6.3 User's Guide, Chapter 7.19: Porous Media Conditions, September 2006.

Fourie W., Said R., Young P., Barnes D.L. 2007. *The simulation of pore scale fluid flow with real world geometries obtained from X-ray computed tomography*. COMSOL Conference, Boston, United States, 14 March.

Gnuplot Home Page. Online: http://www.gnuplot.info/ (access: 1.05.2015).

Hernandez Á.R.Á. 2005. *Combined Flow And Heat Transfer Characterization of Open Cell Aluminum Foams*. MSc Thesis. Mechanical Engineering, University Of Puerto Rico, Mayagez Campus, San Juan, Puerto Rico.

ITASCATM Home Page. Online: http://www.itascacg.com/pfc3d/ (access: 1.05.2015).

Kozeny J. 1927. *Über kapillare Leitung des Wassers im Boden*. Akademie der Wissenschaften in Wien, Sitzungsberichte, 136(2a): 271–306.

Liu Ch., Zhang Q., Chen Y. 2008. *PFC^{3D}* Simulations of lateral pressures in model bin. ASABE International Meeting, paper number 083340. Rhode Island.

Liu Ch., Zhang Q., Chen Y. 2008. *PFC^{3D}* Simulations of vibration characteristisc of bulk solids in storage bins. ASABE International Meeting, paper number 083339. Rhode Island.

Lord D.L., Rudeen D.K., Schatz J.F., Gilkey A.P., Hansen C.W. 2006. *DRSPALL: Spallings Model for the Waste Isolation Pilot Plant 2004 Recertification*. SAND2004-0730, Sandia National Laboratories, Albuquerque, New Mexico, Livermore, California.

Mian M.A. 1992. *Petroleum engineering handbook for the practicing engineer*. Pennwell Publishing, Tulsa, Oklahoma.

Neethirajan S., Karunakaran C., Jayas D.S., White N.D.G. 2006. *X-ray Computed Tomography Image Analysis to explain the Airflow Resistance Differences in Grain Bulks*. Biosystems Engineering, 94(4): 545–555.

Niven R.K. 2002. *Physical insight into the Ergun and Wen and Yu equations for fluid flow in packed and fluidised beds*. Chemical Engineering Science, 57(3): 527–534.

ParaView Home Page. Online: http://www.paraview.org/ (access: 1.05.2015).

Rainey T.J., Doherty W.O.S., Brown R.J., Kelson N.A., Martinez D.M. 2008. *Determination of the permeability parameters of bagasse pulp from two different sugar extraction methods*. TAPPI Engineering, Pulping & Environmental Conference. Portland, Oregon, United States, August 24–27.

Resch E. 2008. *Numerical and Experimental Characterisation of Convective Transport in Solid Oxide Fuel Cells*. MSc Thesis, Queens University, Kingston, Ontario, Canada.

Rossel S.M. 2004. *Fluid flow modeling of resin transfer molding for composite material wind turbine blade structures*. Sandia National Laboratories on-line report no SAND04-0076. Department of Chemical Engineering, Montana State University – Bozeman, Bozeman, Montana.

Samsuri A., Sim S.H., Tan C.H. 2003. *An Integrated Sand Control Method Evaluation*. Society of Petroleum Engineers, SPE Asia Pacific Oil and Gas Conference and Exhibition, Jakarta, Indonesia, 9–11 September.

Skjetne E., Klov T., Gudmundsson J.S. 1999. *High-Velocity Pressure Loss In Sandstone Fractures: Modeling And Experiments (SCA-9927)*. International Symposium of the Society of Core Analysts, Colorado School of Mines, Colorado, August 1–4.

Sobieski W. 2009a. *Calculating tortuosity in a porous bed consisting of spherical particles with known sizes and distribution in space*. Research report 1/2009, Winnipeg.

SOBIESKI W. 2009b. *Switch Function and Sphericity Coefficient in the Gidaspow Drag Model for Modeling Solid-Fluid Systems*. Drying Technology, 27(2): 267–280.

SOBIESKI W. 2010. *Examples of Using the Finite Volume Method for Modeling Fluid-Solid Systems*. Technical Sciences, 13: 256–265.

SOBIESKI W. 2014. *The quality of the base knowledge in a research process*. Scientific researches in the department of mechanics and machine design, University of Warmia and Mazury in Olsztyn, 2: 29–47.

SOBIESKI W., LIPINSKI S. *The PathFinder User's Guide*. Online: http://www.uwm.edu.pl/pathfinder/ (access: 1.05.2015).

SOBIESKI W., TRYKOZKO A. 2011. *Sensitivity aspects of Forchheimer's approximation*. Transport in Porous Media, 89(2): 155–164.

SOBIESKI W., TRYKOZKO A. 2014a. *Forchheimer Plot Method in Practice*. Part 1. *The experiment*. Technical Sciences, 17(4): 221–335.

SOBIESKI W., TRYKOZKO A. 2014b. *Forchheimer Plot Method in Practice*. Part 2. *A numerical model*. Technical Sciences, 17(4): 337–350.

SOBIESKI W., ZHANG Q., LIU C. 2012. *Predicting Tortuosity for Airflow Through Porous Beds Consisting of Randomly Packed Spherical Particles*. Transport in Porous Media, 93(3): 431–451.

The MayaVi Data Visualizer. Online: http://mayavi.sourceforge.net/index.html (access: 1.05.2015).

The PathFinder Project. Online: http://www.uwm.edu.pl/pathfinder/ (access: 1.05.2015).

WHITAKER S. 1996. *The Forchheimer equation: A theoretical development*. Transport in Porous Media, 25(1): 27–61.

WU J., YU B., YUN M. 2008. *A resistance model for flow through porous media*. Transport in Porous Media, 71(3): 331–343.